MATTER: International Journal of Science and Technology
ISSN 2454-5880

Al-Gizi et al., 2017

Volume 3 Issue 3, pp. 36-50

Date of Publication: 15th November 2017

DOI-https://dx.doi.org/10.20319/mijst.2017.32.3650

This paper can be cited as: Al-Gizi, A., Al-Chlaihawi, S., & Craciunescu, A. (2017). Comparative Study of Some FLC-Based MPPT Methods for Photovoltaic Systems. MATTER: International Journal of Science and Technology, 3(3), 36-50.

COMPARATIVE STUDY OF SOME FLC-BASED MPPT METHODS FOR PHOTOVOLTAIC SYSTEMS

Ammar Al-Gizi
Electrical Engineering Faculty, University Politehnica of Bucharest, Romania
ammar.ghalib@yahoo.com

Sarab Al-Chlaihawi
Electrical Engineering Faculty, University Politehnica of Bucharest, Romania
sarab.haedar@yahoo.com

Aurelian Craciunescu
Electrical Engineering Faculty, University Politehnica of Bucharest, Romania
aurelian.craciunescu@upb.ro

Abstract

In this paper, an asymmetrical and symmetrical fuzzy logic controller (FLC) based maximum power point tracking (MPPT) methods are compared. The input membership function (MF) setting values are calculated based on the power-voltage (P-V) characteristics of the utilized photovoltaic (PV) module at standard technical conditions (STC). Moreover, five and seven triangular (5-tri and 7-tri) MFs are analyzed. The performance comparisons of the different categories of the FLC-based PV MPPT methods are performed using Matlab/Simulink package. A BP SX150S PV module is used in the simulation at STC. According to the simulation results, the asymmetrical FLC-based MPPT method has the superior results in terms of transient and

steady state tracking performances for the different numbers of MFs. In the case of 5-tri MFs, the asymmetrical FLC-based MPPT method can enhance the rising time (t_r), tracking accuracy, and energy yield by 84%, 0.05%, and 13.25% respectively, compared to the symmetrical FLC. Whereas, in the case of 7-tri MFs, the rising time, tracking accuracy, and extracted energy are enhanced by 86.7%, 0.04%, and 14.72% respectively. The rising time and extracted energy are improved approximately by 10% and 0.08%, respectively, by using 7-tri MFs in the asymmetrical FLC. Consequently and regardless of the number of MFs, the asymmetrical FLC can be used as the most promising MPPT method for improving the overall performance of the PV system.

Keywords

Photovoltaic Systems, Maximum Power Point Tracking, Fuzzy Logic Controller, Perturb and Observe

1. Introduction

In recent years, many studies are proposed to increase the efficiency of the photovoltaic (PV) system, thereby harvesting maximum solar energy to the load (Afandi & Chandrarini, 2015) (Charan, Laxmi, & Sangeetha, 2017). For this purpose, various maximum power point tracking (MPPT) methods like perturb and observe (P&O) and incremental conductance (InC) were used in the literature. The using of these methods usually leads to a loss of energy due to its oscillation around the maximum power point (MPP) (Subudhi & Pradhan, 2013) (Eltawil & Zhao, 2013). Nowadays, the MPPT based on the fuzzy logic (FL) is widely used to find and track the MPP for the PV system due to its effectiveness and adaptability to a complex system (Bendib, Krim, Belmili, Almi, & Boulouma, 2014). In the literature, various combinations of FLC with ANN (Al-Gizi, Craciunescu, & Al-Chlaihawi, 2017) and FLC with PSO (Rahma & Khemliche, 2014) were proposed for improving the overall performance of PV system. Where, the FLC-based MPPT including five membership functions (MFs) of triangular shapes was used.

The definition of MFs and rules represents a major part in the design of FLC. For conventional FLC, the MFs are usually defined by the trial and error which does not maintain the required results (Islam, Talukdar, Mohammad, & Khan, 2010).

In this article, a symmetrical and an asymmetrical FL-based MPPT controllers are proposed, taken into consideration five and seven triangular MFs. Moreover, the conventional

P&O which is developed in (Attou, Massoum, & Chadli, 2015) is also presented to highlight the improvements of the proposed FLC-based MPPT methods. The PV system modeling is explained in section 2; the FLC-based MPPT is described in section 3. Meanwhile, the simulation results are discussed in section 4. Finally, the conclusion and future works are disclosed in section 5.

2. Modeling of the PV System

The main components of a typical stand-alone PV system can be represented by PV module, load, and MPPT control system including dc-dc converter and MPPT algorithm, as shown in Fig. 1.

In this article, the following types are used:

- BP SX150S PV module consisting (N_S=72) series-connected solar cells.
- Constant resistive load (R_L=6Ω).
- Ideal buck-boost dc-dc converter.
- P&O and FLC-based MPPT methods

The utilized BP SX150S PV module is capable of providing a maximum output power of 150 W under standard technical condition (STC). At STC, the temperature T_r is 298 ^{o}K or 25 ^{o}C and the solar irradiation G_r is 1000 W/m^2 at the air mass (AM=1.5). Table 1 lists the electrical parameters of the utilized PV module (Al-Gizi et al., 2017).

The main purpose of the dc-dc converter is maintaining the matching between the input impedance of the converter (R_{in}) and the PV optimal impedance (R_{opt}) for locating the operating point at MPP, thereby extracting a maximum available power from the PV module (Al-Gizi, 2016). R_{opt} can be represented by:

$$R_{opt} = \frac{V_{MPP}}{I_{MPP}} \qquad (1)$$

Where, V_{MPP} and I_{MPP} are voltage and current of PV module at the MPP, respectively.

Based on the utilized ideal dc-dc converter, the relationship between R_{in}, load impedance (R_L), and duty cycle (D) can be described by:

$$R_{in} = \frac{V}{I} = \frac{(1-D)^2}{D^2} \times \frac{V_L}{I_L} = \frac{(1-D)^2}{D^2} \times R_L \qquad (2)$$

Where V and I are the voltage and current of the PV module, whereas, V_L and I_L are voltage and current of the load, respectively.

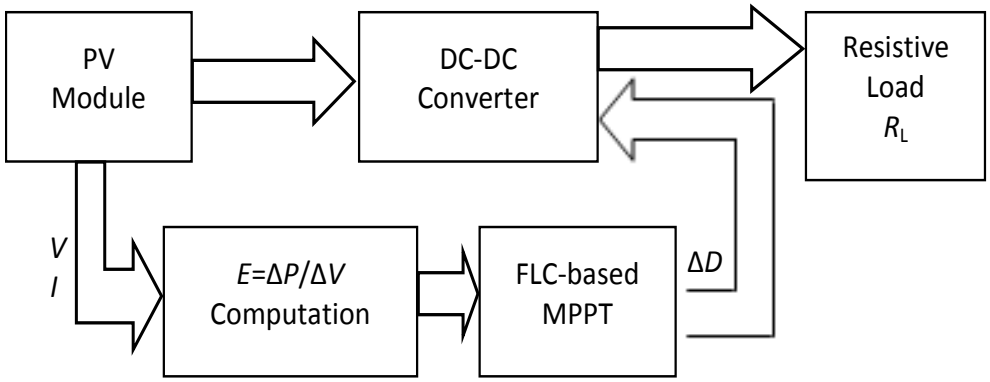

Figure 1: *Photovoltaic system with FLC-based MPPT method*

Table 1: *Electrical parameters of BP SX 150S PV module at STC*

Parameter	Value
Maximum Power (P_{max})	150 W
Voltage at P_{max} (V_{MPP})	34.5 V
Current at P_{max} (I_{MPP})	4.35 A
Short-circuit current (I_{sc})	4.75 A
Open-circuit voltage (V_{oc})	43.5 V
Temperature coefficient of I_{sc}	(0.065 ± 0.015) %/ ^{o}C
Temperature coefficient of V_{oc}	−(160 ± 20) mV/ ^{o}C
Temperature coefficient of power	−(0.5 ± 0.05) %/ ^{o}C

It can be seen from (2), by controlling the value of duty cycle (D), the load matching can be maintained. By increasing D, R_{in} will be decreased; hence, the operating point will be moved in an anti-clockwise direction (i.e. module voltage will be decreased) and vice versa.

Based on the PV cell of a single-diode model, the operating point of the PV module represented by it's current (I) and voltage (V) at different values of solar irradiance (G), and cell temperature (T), can be described by the following characteristic equation:

$$I = f(V,G,T) = I_{ph} - I_o\left(\exp\left(\frac{q(V+IR_s)}{N_s n\, KT}\right)-1\right)-\left(\frac{V+IR_s}{R_{sh}}\right) \qquad (3)$$

In terms of R_{in}, I-V equation can be written as:

$$V - R_{in} I = V - R_{in}\, f(V,G,T) = 0 \qquad (4)$$

Where I_{ph} is a light current or a short-circuit current which is denoted by I_{sc}. I_o is the diode's reverse saturation current, q is the electron charge (1.602×10^{-19} C), K is the Boltzmann's constant (1.381×10^{-23} J/K), and n is the diode ideality factor (sometimes denoted as "A") (1.62 in this article). R_s and R_{sh} are the series and parallel resistances of the PV cell (Bellia, Ramdani, Moulay, & Medles, 2013) (Papadopoulou, 2013). The relationship between I_o and T can be represented by:

$$I_o = I_{or} \times \left(\frac{T}{T_r}\right)^3 \times \exp\left(\frac{q\,E_g}{n\,K}\left(\frac{1}{T_r} - \frac{1}{T}\right)\right) \qquad (5)$$

Where E_g is the band gap energy of the cell's semiconductor. On the other hand, the dependency of I_{sc} on T and G can be shown by:

$$I_{sc} = \frac{G}{G_r}\left(I_{scr} + \alpha(T - T_r)\right) \qquad (6)$$

Where α is the short circuit current temperature coefficient.

By increasing the value of D from 0 to 1 and solving the mathematical equations (2), (3), and (4), using Newton's numerical iterative method, the curves of power change (ΔP), voltage change (ΔV), and corresponding $\Delta P/\Delta V$ can be concluded. These curves are shown in Fig. 2, Fig. 3 and Fig. 4, respectively, at different values of G and constant T of 25 ^{o}C.

The value of an optimal D is dependent on the utilized MPPT control algorithm.

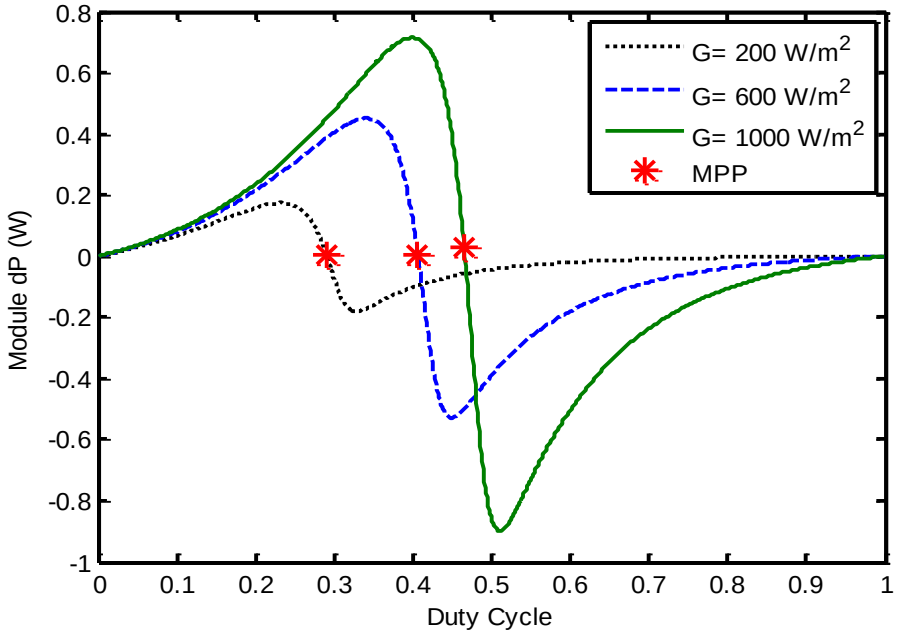

Figure 2: *ΔP curves of the PV module at different irradiations and 25 ^{o}C of temperature*

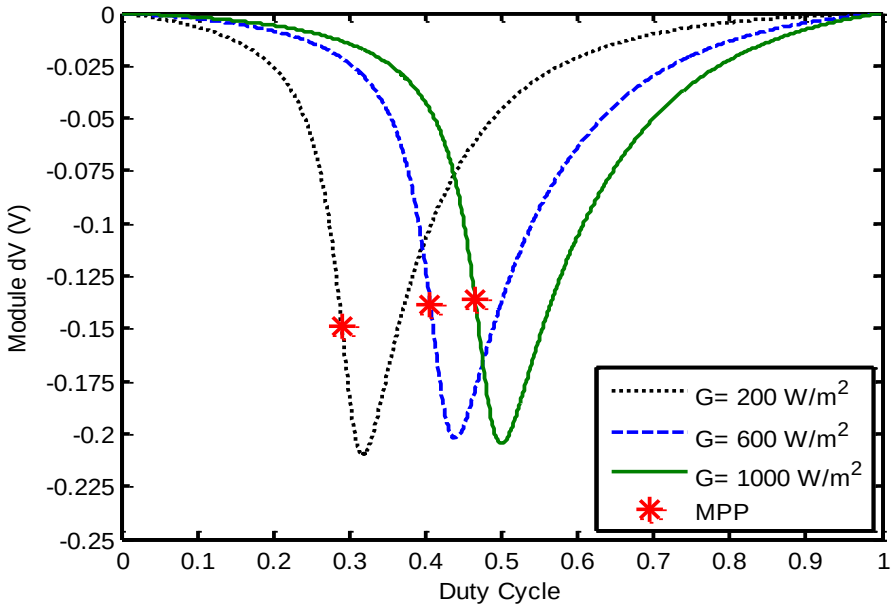

Figure 3: *ΔV curves of the PV module at different irradiations and 25 °C of temperature*

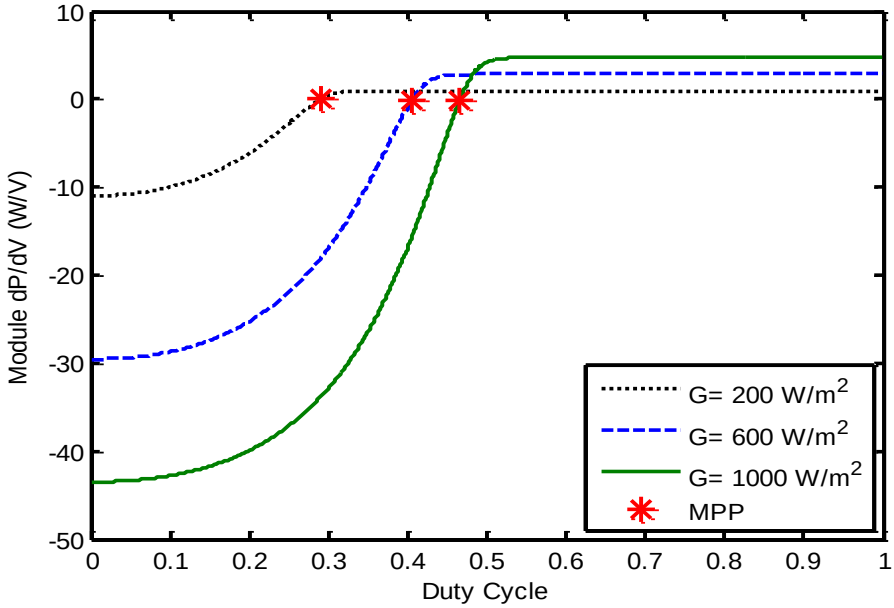

Figure 4: *ΔP/ΔV curves of the PV module at different irradiations and 25 °C of temperature*

3. FLC-based MPPT Method

The fuzzy logic control (FLC) is used to convert a complex problem to a list of rules and solving it without needing to use a mathematical model (Bendib et al., 2014). The FLC-based MPPT is used to adjust the duty cycle (*D*) of the dc-dc converter to maintain the MPP. The structure of FLC is shown in Fig. 5.

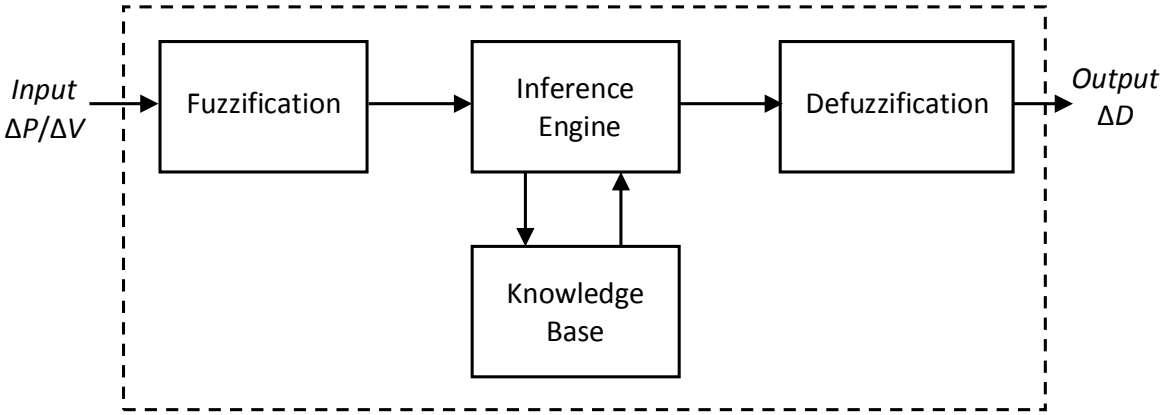

Figure 5: *Structure of the fuzzy logic controller (FLC)*

In this article, the input and output variables of the proposed FLC are the power slope ($\Delta P/\Delta V$) and the duty cycle variation (ΔD), respectively. Meanwhile, five and seven MFs are used to represent the FLC's input and output variables with linguistic terms: positive (*P*), negative (*N*), zero (*Z*), small (*S*), medium (*M*), and big (*B*).

In the case of five MFs, the corresponding FLC's rule base (RB) includes five rules, as shown in Table 2. In contrast, in the case of seven MFs, the rules are seven, as shown in Table 3. These rules are set based on a location of the operating point with the MPP. If the operating point converges to the MPP, ΔD will be slightly increased or decreased and vice versa, to attain the MPP.

The control rules can be easily illustrated by observing $\Delta P/\Delta V$ curve under STC which is shown in Fig. 6.

Table 2: *Rules of FLC of five MFs*

ΔP/ΔV	*NB*	*NS*	*Z*	*PS*	*PB*
ΔD	*PB*	*PS*	*Z*	*NS*	*NB*

Table 3: *Rules of FLC of seven MFs*

ΔP/ΔV	*NB*	*NM*	*NS*	*Z*	*PS*	*PM*	*PB*
ΔD	*PB*	*PM*	*PS*	*Z*	*NS*	*NM*	*NB*

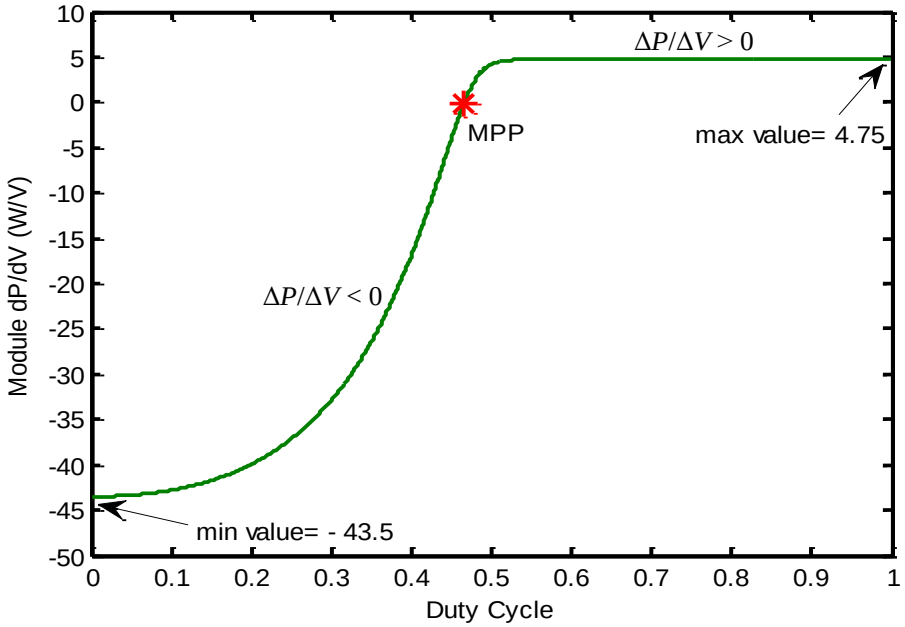

Figure 6: *ΔP/ΔV curve of the PV module at STC*

According to a defuzzification stage of the FLC shown in Fig. 5, the center of gravity (COG) method is used to produce the crisp value of ΔD as:

$$\Delta D = \frac{\sum_{i=1}^{n} \Delta D_i \times \mu(\Delta D_i)}{\sum_{i=1}^{n} \mu(\Delta D_i)} \qquad (7)$$

Where $\mu(\Delta D_i)$ is the fuzzy output of inference engine at rule i, ΔD_i is the corresponding crisp output of rule i, n is a number of rules (5 and 7 in the case of five and seven rules, respectively). Whereas ΔD is a final crisp value of the FLC's output. Consequently, based on the produced ΔD, the actual duty cycle (D) of the dc-dc converter can be adjusted (Al-Gizi, 2016).

The definition of MFs' parameters influences on the performance of the FLC-based MPPT (Rahma & Khemliche, 2014). Hence, in this article, symmetrical and asymmetrical FLC is used taking into consideration five and seven triangular MFs in the FLC's input and output.

3.1 Symmetrical FLC

Fig. 7 shows MFs of the input $\Delta P/\Delta V$ for the symmetrical FLC, using five and seven triangular MFs. Where, the maximum negative and positive values of $\Delta P/\Delta V$ are chosen as -43.5 and 43.5, respectively.

According to the output ΔD of FLC, however, a large value of ΔD leads to improve the transient response represented by the tracking speed, in contrast, the ripple on the steady-state will be increased, and vice versa. In this article, the maximum negative and positive values of ΔD are set as -0.05 and 0.05, respectively.

The MFs of ΔD for the symmetrical FLC, using five and seven triangular MFs, are shown in Fig. 8.

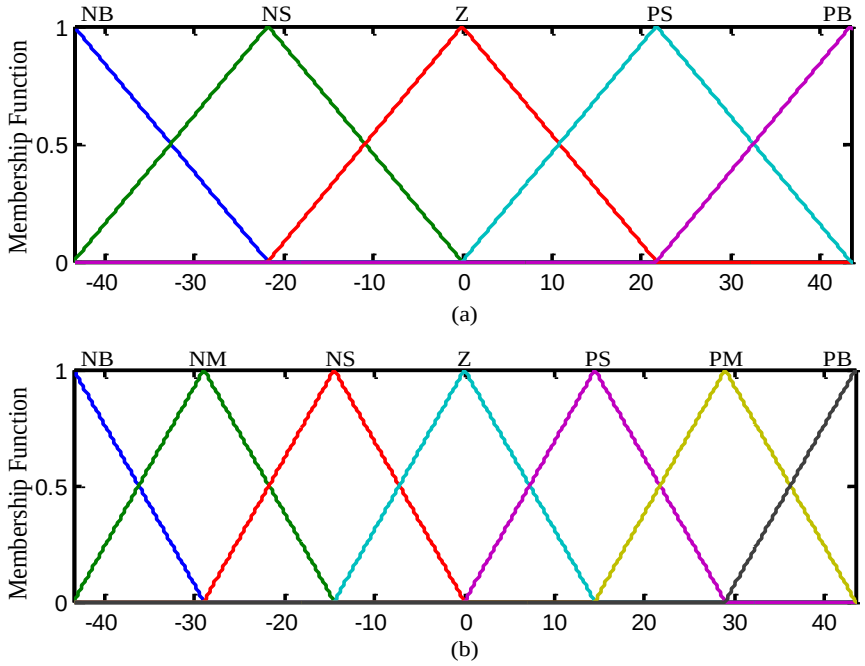

Figure 7: *Input $\Delta P/\Delta V$ of the symmetrical FLC: (a) 5-MFs; (b) 7-MFs*

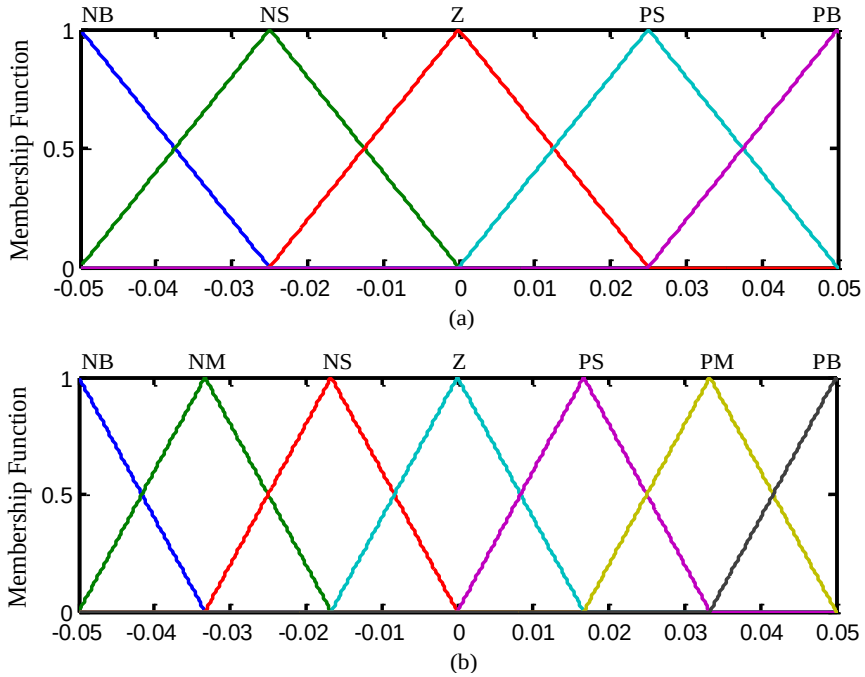

Figure 8: *Output ΔD of the symmetrical FLC: (a) 5-MFs; (b) 7-MFs*

3.2 Asymmetrical FLC

The parameters of the asymmetrical MFs under STC can be determined by observing Fig. 6. Since the values of $\Delta P/\Delta V$ on the right-side of MPP is larger than its values on the left-side at a fixed ΔD. Therefore, based on the fixed symmetrical MFs of ΔD shown in Fig. 8, the maximum negative and positive values of $\Delta P/\Delta V$ are set by -43.5 and 4.75, respectively. Fig. 9 shows MFs of $\Delta P/\Delta V$ for the asymmetrical FLC, using five and seven triangular MFs.

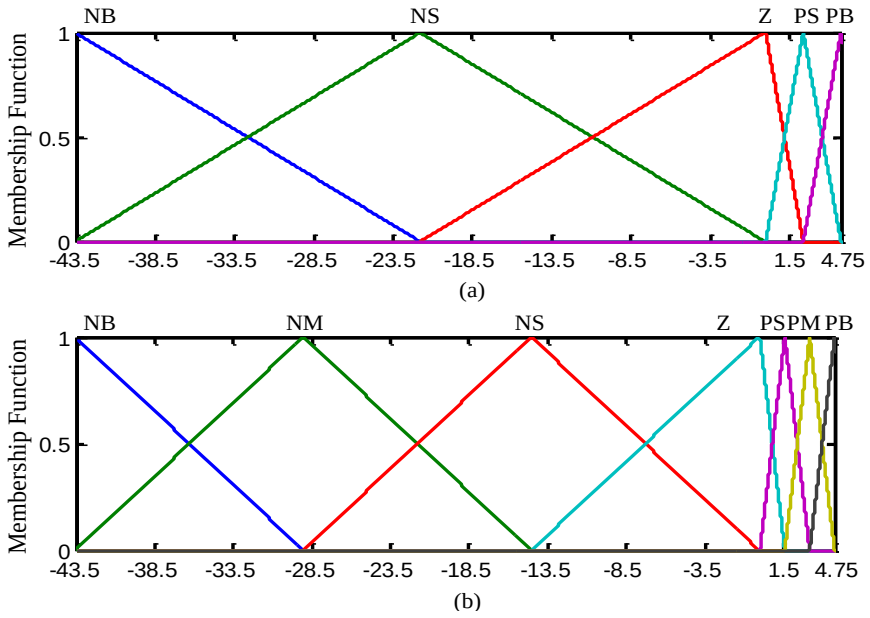

Figure 9: *Input $\Delta P/\Delta V$ of the asymmetrical FLC: (a) 5-MFs; (b) 7-MFs*

4. Simulation Results and Discussion

The Matlab simulation results are evaluated for P&O, symmetrical, and asymmetrical FLC-based MPPT methods under STC, during the 30s period of time. Where, the flow chart of the FLC-based MPPT method is shown in Fig. 10. The initial operating point is chosen at the left-side of the MPP by using the initial duty cycle (D) of 0.9.

In this article, the simulation results of the different MPPT methods are compared in terms of three indices: steady state accuracy, extracted energy, and rising time t_r. These indices can be defined as follows:

$$\text{Steady-state Accuracy (\%)} = \frac{P_{av}}{P_{MPP}} \times 100 = \frac{\int_{t_r}^{t_f} V \cdot I \, dt}{\int_{t_r}^{t_f} P_{MPP} \, dt} \times 100 \qquad (8)$$

$$\text{Extracted Energy (Wh)} = \frac{\int_0^{t_f} P(t)\,dt}{3600} \quad (9)$$

Where, P_{av} is the average steady-state output power; P_{MPP} is the average maximum power at MPP, P(t) is the instantaneous power at time t, t_f is the final simulation time (the 30 s in this article), and t_r is the rising time which is the time required for the output power to go from 10% to 90% of its final value (Harrag & Messalti, 2015).

The output power delivered from the utilized module using different MPPT methods are illustrated in Fig. 11 using five triangular MFs. In contrast, Fig. 12 shows the power performances in case of using seven MFs. Moreover, Table 4 summarizes the performance comparisons of the three MPPT methods.

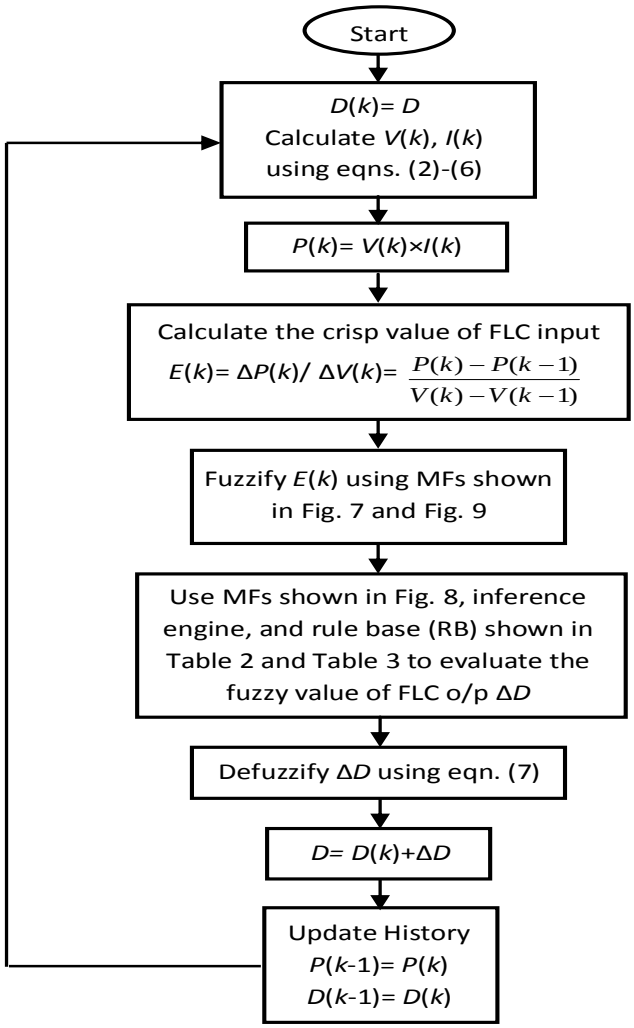

Figure 10: *Flow chart of the FLC-based PV MPPT method*

Fig. 11 and Fig. 12 clearly show that the symmetrical FLC-based MPPT method provides a better transient and steady-state performances than the conventional P&O method. Furthermore, the asymmetrical FLC-based MPPT method of five and seven MFs can provide better performance than P&O and symmetrical FLC.

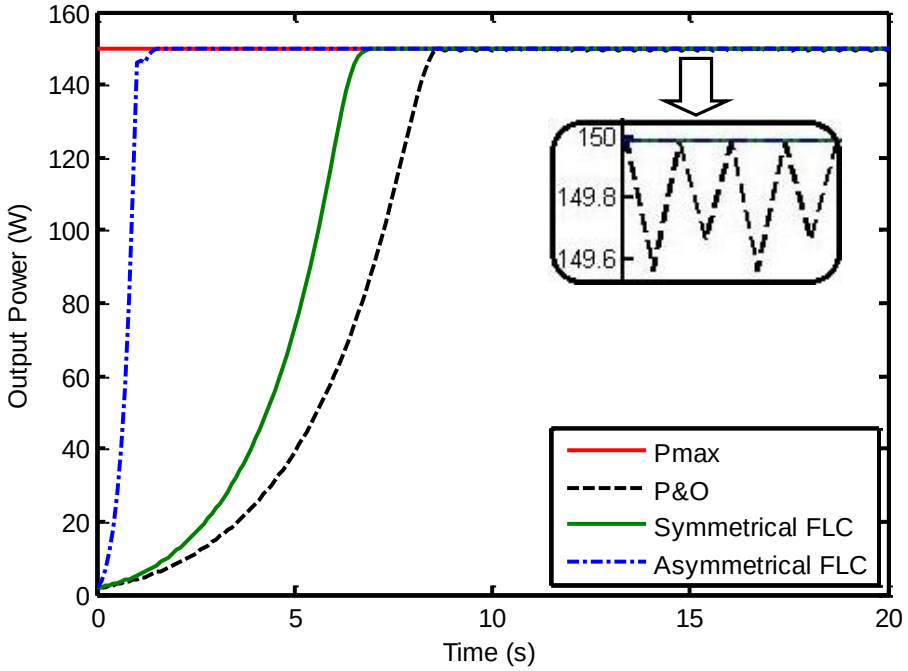

Figure 11: *Power performances using MPPT methods at STC with five MFs*

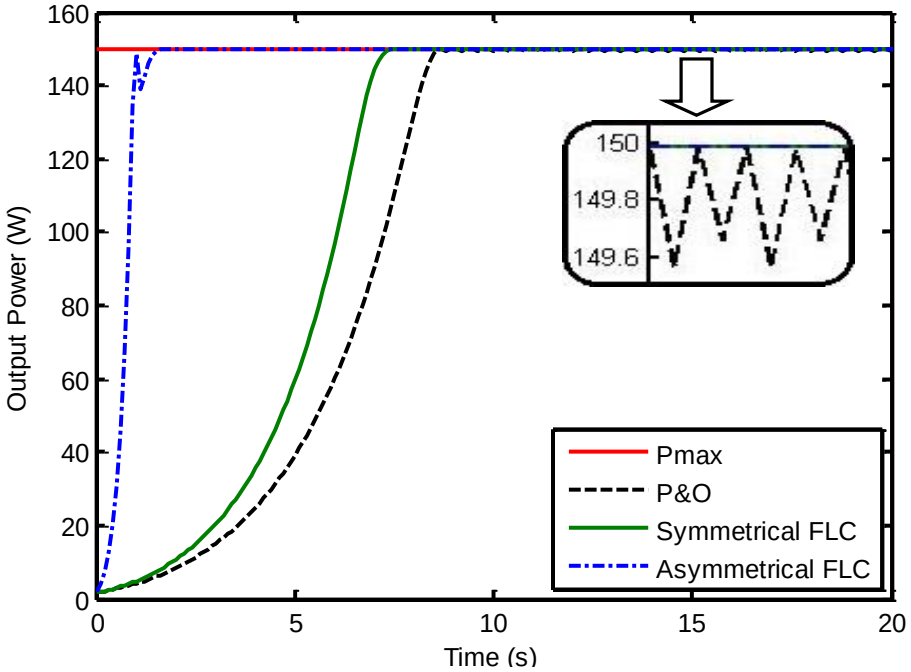

Figure 12: *Power performances using MPPT methods at STC with seven MFs*

In the case of five MFs, the asymmetrical FLC is capable of reaching the MPP by a rising time t_r of 1 s with an accuracy of 99.97%. Consequently, the available extracted energy from the utilized PV module is 1.222 Wh. Whereas, by using symmetrical FLC, t_r, accuracy, and extracted energy are 6.3 s, 99.92%, and 1.06 Wh, respectively, as shown in Fig. 11 and Table 4.

In contrast, the asymmetrical FLC of seven MFs can reach the MPP by t_r of 0.9 s with an accuracy of 99.94%. Hence, the energy of 1.223 Wh can be extracted from the PV module. Whereas, t_r, accuracy, and extracted energy are 6.8 s, 99.9%, and 1.043 Wh, respectively, by using symmetrical FLC, as shown in Fig. 12 and Table 4.

In the same manner, the asymmetrical FLC of seven MFs is better than that of five MFs in terms of rising time and extracted energy. Where, t_r are 0.9 s and 1 s using asymmetrical FLC of seven and five MFs, respectively. Whereas, maximum energies which can be extracted from the PV module using asymmetrical FLC of seven and five MFs are 1.223 Wh and 1.222 Wh, respectively, as shown in Table 4.

Table 4: *Performance results of MPPT methods at STC*

MPPT Algorithms	Average Steady-State Power[1] (W)	Steady-State Accuracy (%)	Rising Time t_r (s)	Extracted Energy[2] (Wh)
P&O (ΔD=0.005)	149.64	99.77	8.1	1
Symmetrical FLC (5MFs)	149.87	99.92	6.3	1.06
Asymmetrical FLC (5MFs)	149.94	99.97	1	1.222
Symmetrical FLC (7MFs)	149.84	99.90	6.8	1.043
Asymmetrical FLC (7MFs)	149.90	99.94	0.9	1.223

[1] The ideal module output power at MPP (P_{MPP}) is 149.9873 W.
[2] The ideal extracted energy is 1.25 Wh.

5. Conclusion and Future Works

This article presents a symmetrical and an asymmetrical FLC-based MPPT methods using five and seven triangular MFs. The performances of these methods are evaluated and compared with the conventional P&O under STC based on three indices defined by accuracy, rising time t_r, extracted energy thereby exploring the best MPPT method.

Asymmetrical FLC-based MPPT method of five and seven MFs have superior results compared with the other MPPT methods. It provides the highest accuracy, extracted energy, and lowest t_r, as shown in Fig. 11, Fig. 12, and Table 4. Furthermore, it can be concluded that the asymmetrical FLC-based MPPT method of seven MFs has better performances than that of five MFs in terms of rising time and extracted energy. Where, rising time and extracted energy are improved by 10% and 0.08%, respectively, as shown in Table 4. In general and regardless of the number of MFs, the asymmetrical FLC can significantly be used as the most promising MPPT method for improving the overall performance of the PV system.

In the future works, the optimization of parameters and types of FLC MFs have to be taken into consideration. Also, another intelligent PV MPPT algorithm should be explored.

References

Afandi, M. M., & Chandrarini, D. D. (2015). Optimization of solar energy utilization using concentrated solar hybrid energy harvester (CSHEH) based on smart solar panel and concentrated thermoelectric generator. *MATTER: International Journal of Science and Technology*, *1*(1), 64-75. https://doi.org/10.20319/mijst.2016.s11.6475

Al-Gizi, A. G. (2016). Comparative study of MPPT algorithms under variable resistive load. *2016 International Conference on Applied and Theoretical Electricity (ICATE)*, 1-6. https://doi.org/10.1109/ICATE.2016.7754611

Al-Gizi, A. G., Craciunescu, A., & Al-Chlaihawi, S. J. (2017). The use of ANN to supervise the PV MPPT based on FLC. *2017 10th International Symposium on Advanced Topics in Electrical Engineering (ATEE)*, 703-708. https://doi.org/10.1109/ATEE.2017.7905128

Attou, A., Massoum, A., & Chadli, M. (2015). Comparison study of two tracking methods for photovoltaic systems. *Rev. Roum. Sci. Techn.–Électrotechn. et Énerg*, *60*(2), 205-214.

Bellia, A. H., Ramdani, Y., Moulay, F., & Medles, K. (2013). Irradiance and temperature impact on photovoltaic power by design of experiments. *Rev. Roum. Sci. Techn.–Électrotechn. et Énerg*, *58*(3), 284-294.

Bendib, B., Krim, F., Belmili, H., Almi, M., & Boulouma, S. (2014). Advanced fuzzy MPPT controller for a stand-alone PV system. *Energy Procedia*, *50*, 383-392. https://doi.org/10.1016/j.egypro.2014.06.046

Charan, C. R., Laxmi, A. J., & Sangeetha, P. (2017). Optimized energy efficient solution with stand alone PV system. *MATTER: International Journal of Science and Technology*, *3*(1), 16-27. https://doi.org/10.20319/Mijst.2017.31.1627

Eltawil, M. A., & Zhao, Z. (2013). MPPT techniques for photovoltaic applications. *Renewable and Sustainable Energy Reviews*, *25*, 793-813. https://doi.org/10.1016/j.rser.2013.05.022

Harrag, A., & Messalti, S. (2015). Variable step size modified P&O MPPT algorithm using GA-based hybrid offline/online PID controller. *Renewable and Sustainable Energy Reviews*, *49*, 1247-1260. https://doi.org/10.1016/j.rser.2015.05.003

Islam, M. A., Talukdar, A. B., Mohammad, N., & Khan, P. K. (2010). Maximum power point tracking of photovoltaic arrays in Matlab using fuzzy logic controller. *2010 Annual IEEE India Conference (INDICON)*, 1-4. https://doi.org/10.1109/INDCON.2010.5712680

Papadopoulou, E. (2013). *Photovoltaic Industrial Systems An Environmental Approach*. Berlin: Springer Berlin. https://doi.org/10.1007/978-3-642-16301-2

Rahma, A., & Khemliche, M. (2014). Combined approach between FLC and PSO to find the best MFs to improve the performance of PV system. *2014 International Conference on Electrical Sciences and Technologies in Maghreb (CISTEM)*, 1-8. https://doi.org/10.1109/CISTEM.2014.7077038

Subudhi, B., & Pradhan, R. (2013). A comparative study on maximum power point tracking techniques for photovoltaic power systems. *IEEE Transactions on Sustainable Energy*, *4*(1), 89-98. https://doi.org/10.1109/TSTE.2012.2202294